Nanoscale Research Letters
a SpringerOpen Journal

NANO EXPRESS Open Access

# Energy absorption ability of buckyball $C_{720}$ at low impact speed: a numerical study based on molecular dynamics

Jun Xu[1], Yibing Li[2], Yong Xiang[3*] and Xi Chen[1,4,5*]

**Abstract**

The dynamic impact response of giant buckyball $C_{720}$ is investigated by using molecular dynamics simulations. The non-recoverable deformation of $C_{720}$ makes it an ideal candidate for high-performance energy absorption. Firstly, mechanical behaviors under dynamic impact and low-speed crushing are simulated and modeled, which clarifies the buckling-related energy absorption mechanism. One-dimensional $C_{720}$ arrays (both vertical and horizontal alignments) are studied at various impact speeds, which show that the energy absorption ability is dominated by the impact energy per buckyball and less sensitive to the number and arrangement direction of buckyballs. Three-dimensional stacking of buckyballs in simple cubic, body-centered cubic, hexagonal, and face-centered cubic forms are investigated. Stacking form with higher occupation density yields higher energy absorption. The present study may shed lights on employing $C_{720}$ assembly as an advanced energy absorption system against low-speed impacts.

**Keywords:** Impact, Energy absorption, Buckyball, Buckling

## Background

Absorption of external impact energy has long been a research topic with the pressing need from civil [1,2] to military needs [3,4]. In particular, effective absorption of mechanical energy at low-impact speed, i.e., below 100 m/s is of great interest [5,6]. As one of the major branches of fullerene family, the carbon nanotube (CNT) has demonstrated an outstanding mechanical energy dissipation ability through water-filled CNT [7], CNT forest and bundle [7], CNT/epoxy nanocomposites [8], CNT immersed in nonaqueous liquid [9], intercalating vertical alignment with aligned existing layered compounds [10], and sponge-like material containing self-assembled interconnected CNT skeletons [11], among others. The advantage lies within the CNTs' intriguing mechanical properties, i.e., ultra-strong (Young's modulus of 0.9 to 5.5 TPa [12-14] and tensile strength of 60 GPa [12]) and ultra-light, as well as the tube structure which buckles upon external loadings [15]. Both theoretical modeling [16-18] and experiments [19-21] have proposed that the energy dissipation density of CNTs could be on the order of 200 J/cm$^3$, about 1-2 order of magnitudes over traditional engineering material [1].

Naturally, another branch of fullerene family with a spherical shape, i.e., the buckyball, also possesses excellent mechanical properties similar to CNTs. Man et al. [22] examined a $C_{60}$ in collision with a graphite surface and found that the $C_{60}$ would first deform into a disk-like structure and then recover to its original shape. It is also known that $C_{60}$ has a decent damping ability by transferring impact energy to internal energy [23,24]. This large deformation ability under compressive strain of $C_{60}$ was also verified by Kaur et al. [25]. For higher impact energy, Zhang [26] employed $C_{60}/C_{320}$ to collide with mono/double layer graphene, and the penetration of graphene and the dissociation of buckyball were observed. Furthermore, Wang and Lee [27] observed a novel phenomenon of heat wave propagation driven by impact loading between $C_{60}$ and graphene which was responsible for the mechanical deformation of the buckyball. Meanwhile, giant buckyballs, such as $C_{720}$, have

* Correspondence: xiang@uestc.edu.cn; xichen@columbia.edu
[3]State Key Lab of Electronic Thin Films and Integrated Devices, School of Energy Science and Engineering, University of Electronic Science and Technology of China, Chengdu, Sichuan 611731, People's Republic of China
[1] Columbia Nanomechanics Research Center, Department of Earth and Environmental Engineering, Columbia University, New York, NY 10027, USA

smaller system rigidity as well as non-recoverable morphology upon impact, and thus they are expected to have higher capabilities for energy dissipation [28]. However, to the best knowledge of the authors, currently, only few studies about the mechanical behavior of giant buckyball are available [29-31].

To understand the mechanical behavior of $C_{720}$ and investigate its energy absorption potential in this paper, the dynamic response of $C_{720}$ is studied at various impact speeds below 100 m/s by employing molecular dynamics (MD) simulations. Firstly, the buckling behaviors under both low-speed crushing and impact are discussed and described using classical thin shell models. Next, 1-D alignment of $C_{720}$ system is investigated to identify the influence of packing of the buckyball on unit energy absorption. Finally, 3-D stacking of $C_{720}$ system is considered, where four types of packing forms are introduced and the relationship between unit energy absorption and stacking density are elucidated by an empirical model.

## Methods

### Computational model and method

The $C_{720}$ is a spherical buckyball with diameter of 2.708 nm (where the van der Waals equilibrium distance is considered), volume of 7.35 $nm^3$, and mass of $1.45 \times 10^{-20}$ g. $C_{720}$ with varying numbers and packing directions (both vertical and horizontal) are selected in this study. Computational cells from single buckyball to 3-D buckyball stacking system are illustrated in selected examples in Figure 1. In the scenario of the impact, the buckyball system subjects to the impact of a top rigid plate with incident energy $E_{\text{impactor}}$, and the initial impact speed is below 100 m/s; in the scenario of crushing, the top rigid plate compresses the buckyball system at a constant speed below 100 m/s. The bottom plate, which is rigid and fixed, serves as a receiver, and the force history it experiences could indicate the energy mitigation capability of the protective buckyball system. The buckyball is not allowed to slip with respect to the impactor and receiver plates. Both the impactor and receiver plates are composed of carbon atoms. The masses of the atoms are varied in the following simulation to set various loading conditions (varying impactor mass), while the interactions between the plates and buckyballs remain as carbon-carbon interaction.

MD simulation is performed based on large-scale atomic/molecular massively parallel simulator platform with the micro-canonical ensembles (NVE) [32] after equilibration. A pairwise Lennard-Jones (L-J) potential term is added to the buckyball potential to account for the steric and van der Waals carbon-carbon interaction

$$U(r_{ij}) = 4\varepsilon_{CC}\left[\left(\frac{\sigma_{CC}}{r_{ij}}\right)^{12} - \left(\frac{\sigma_{CC}}{r_{ij}}\right)^{6}\right] \quad (1)$$

where $\varepsilon_{CC}$ is the depth of the potential well between carbon-carbon atoms, $\sigma_{CC}$ is the finite distance where the carbon-carbon potential is zero, $r_{ij}$ is the distance between the two carbon atoms. Here, L-J parameters for the carbon atoms of the buckyball $\sigma_{CC} = 3.47^{\cdot}A$ and $\varepsilon_{CC}$ = 0.27647 kJ/mol as used in the original parametrization of Girifalco [33] and van der Waals interaction govern in the plate-buckyball interaction. A time integration step of 1 fs is used, and periodical boundary conditions are applied in the *x,y* plane to eliminated the boundary effect.

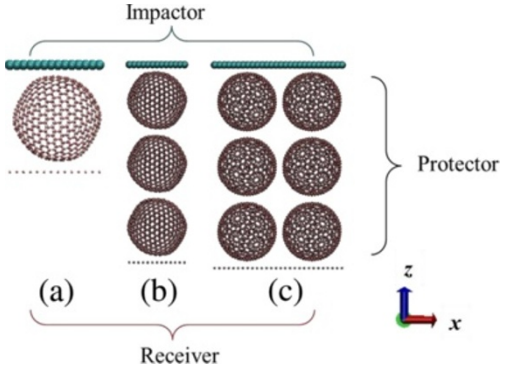


(a) 0-D Single $C_{720}$ buckyball energy absorption system;
(b) 1-D chain-like $C_{720}$ buckyball energy absorption system with 3 buckyballs included
(c) 3-D $C_{720}$ buckyball energy absorption system in Square Cubic (SC) stacking form with 2 by 2 by 3 buckyballs included (*x*-*z* plane side-view)

**Figure 1 Various alignments of buckyball system as a protector.**

## Single buckyball mechanical behavior

### *Atomistic simulation result*

The distinctive mechanical behavior of a single buckyball should underpin the overall energy absorption ability of a buckyball assembly. The force $F$ and displacement $W$ are normalized as $FR/Eh^3$ and $W/D$, respectively, where $R$, $h$, $D$, and $E$ are the radius, effective thickness, diameter, and effective Young's modulus of the buckyball, respectively. Considering that bending is involved during the buckyball compression, $h$ = 0.66 nm and $E$ = 5 TPa [34,35]. Here a crushing speed at 0.01 m/s is employed to mimic quasi-static loading, because the normalized force-displacement curves are verified to be the same at various loading rates from 0.1 to 0.001 m/s in trial simulations. The force-displacement response under both quasi-static and a representative dynamic impact loading (with impact speed of 50 m/s and energy of 1.83 eV) are studied, as shown in Figure 2. Two obvious force-drops could be observed in low-speed crushing, while only one prominent force-drop exists in dynamic loading which is related to the less-evident snap-through deformation shape.

The entire compression process could be divided into four phases according to the $FR/Eh^3 \sim W/D$ curve, i.e., buckling ($W/D$ < 10%), post-buckling (10% ≤ $W/D$ < 30%), densification (30% ≤ $W/D$ < 40%), and inverted-cap-forming phase ($W/D$ > 40%). Upon the ricochet of the plate, the deformation remains as a bowl shape with great volume shrinkage. The stabilization of such a buckled morphology is owing to a lower system potential energy in the buckled configuration due to van der Waals interaction; similar energy dissipation mechanism in CNT network is also revealed by [36].

The derivative of curve undergoes a sudden change at the same $W/D$ value but in two completely different loading rates, suggesting that the sudden force-drop points are highly dependent on the buckyball deformation rather than the loading rate. And theoretical insights may be obtained from the four-phase deformation.

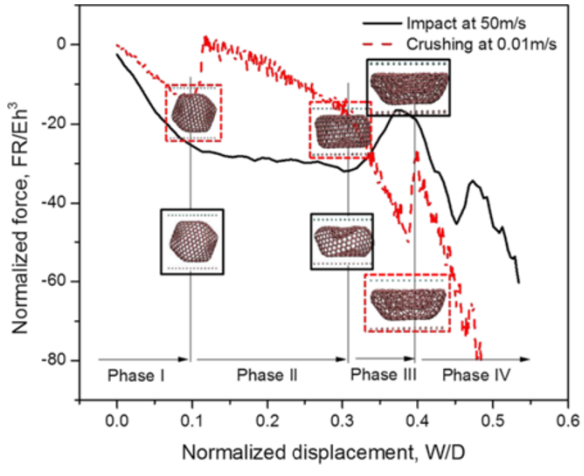


**Figure 2 Normalized force displacement curves at both low-speed crushing and impact loading.** The entire process from the beginning of loading to the bowl-forming morphology can be divided into four phases. Morphologies of $C_{720}$ are shown at the corresponding normalized displacements.

### *Phenomenological mechanical models*

Note that due to the property of $FR/Eh^3 \sim W/D$ curve, among the phases of compression process, those with significant reduction of force (Figure 2) are relatively unimportant for energy absorption and not included in the modeling effort. A three-phase model for low-speed crushing and a two-phase model for impact loading are proposed separately in the following sections.

### *Three-phase model for low-speed crushing (quasi-static loading)*

(1) Phase I. Buckling phase

In the range of small deformation in the beginning of compression, the model describing thin-shell deformation under a point force is applicable [37,38]. Considering a buckyball with wall thickness $h$ = 0.066 nm compressed by $F$ with deformation of $W$ (with the subscript number denoting the phase number sketched in Figure 3), the force-deflection relation should be expressed as [39]

$$F_1 = \frac{8G}{Rc} W_1 \qquad (0 < W_1 \le W_{b1}) \tag{2}$$

where the bending stiffness $G = Ehc^2$; the reduced wall thickness $c = h/\sqrt{12(1-\nu^2)}$ and $\nu$ is the Poisson's ratio. The linear deformation behavior continues until it reaches the critical normalized strain $W_{b1}$. Experimental results for bulk thin spherical shell show that the transition from the flattened to the buckled configuration occurs at a deformation close to twice the thickness of the shell [40]; while $W_{b1}$ here is about 4 $h$, indicating a larger buckling strain in nanoscale structure.

The nanostructure has higher resistance to buckle than its continuum counterpart and based on the fitting of MD simulation, a coefficient $f^* \approx 2.95$ should be expanded to Equation 2 as

$$F_1 = \frac{8G}{Rc} W_1 \cdot (f^*) (0 < W_1 \le W_{b1}) \tag{3}$$

It is reminded that this equation is only valid for $C_{720}$ under low-speed (or quasi-static) crushing.

(2) Phase II. Post-buckling phase

As the compression continues, buckyball continues to deform. Once the compressive strain reaches $W_{b1}$, the flattened area becomes unstable and within a small

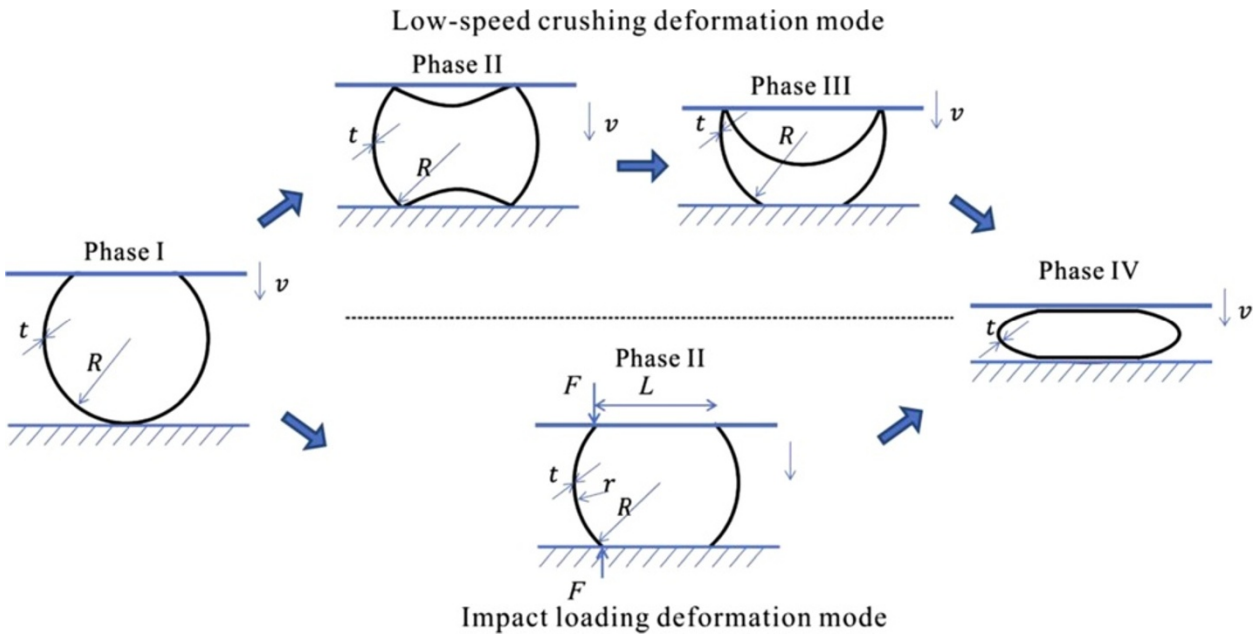


**Figure 3 Illustration of deformation phases during compression for $C_{720}$.** Dynamic loading and low-speed crushing share the same morphologies in phase I while they are different in phase II. Analytical models are based on the phases indicated above and below the dash line for low-speed crushing and impact loading, respectively.

region, the buckyball snaps through to a new configuration in order to minimize the strain energy of the deformation, shown in Figure 3. The ratio between the diameter and thickness of buckyball is quite large, i.e., $D/h \approx 36.5$, and only a small portion of volume is involved thus the stretching energy is of secondary order contribution to the total strain energy. Hubbard and Stronge [41] developed a model to describe the post-buckling behavior of a thin spherical shell under compression based on Steele's [42] model

$$F_2 = \sqrt{\frac{2W_2h}{K}}\frac{16G}{Rc}\left(W_{b1} < W_2 \le W_{b2}\right) \tag{4}$$

where $K = \left(\frac{5}{4}\right)^2\left(\frac{8}{3\pi}\right)^2\sqrt{3(1-\nu^2)}$. This nonlinear deformation behavior extends until it reaches the densification critical normalized strain $W_{b2}$. The value of $W_{b2}$ could be fitted from the simulation data for $C_{720}$ where $W_{b2} \approx 11h$.

The first force-drop phenomenon is obvious once the buckling occurs where the loading drops to nearly zero. Therefore, by applying the boundary condition of $F_2(W_2) \approx 0$, Equation 4 maybe further modified as

$$F_2 = \sqrt{\frac{2h}{K}}\frac{16G}{Rc}\left(\sqrt{W_2} - \sqrt{W_{b2}}\right)\cdot(f^*) \quad \left(W_{b1} < W_2 \le W_{b2}\right) \tag{5}$$

(3) Phase III. Densification phase

When the compression goes further, the crushing displacement eventually becomes much larger than the thickness and thus the force-displacement relation becomes nonlinear [42]. The buckled buckyball is densified during this process. A phenomenological nonlinear spring-like behavior could be fitted as

$$F_3 = \gamma W_3^n, \tag{6}$$

where $\gamma$ is a coefficient and $n$ is fitted as $n \approx 1.16$. Considering the relationship [41,42]

$$\frac{2W_3}{h} = K\left(\frac{F_b}{2}\right)^n \tag{7}$$

and

$$F_b = \frac{F_3R}{8G}\frac{c}{h}, \tag{8}$$

we may come to the equation

$$F_3 = \frac{16Gh}{Rc}\left(\frac{2}{Kh}\right)^n W_3^n \quad \left(W_{b2} < W_3\right) \tag{9}$$

Thus, by considering the continuity of two curves in adjacent phases, we may rewrite Equation 9 as

$$F_3 = \left(\frac{16Gh}{Rc}\left(\frac{2}{Kh}\right)^n \left(W_3^n - W_{b2}^n\right) + F_2(W_{b2})\right)\cdot(f^*)(W_{b2} < W_3) \tag{10}$$

Therefore, Equations 3, 5, and 10 together serve as the normalized force-displacement model which may be used to describe the mechanical behavior of the buckyball under quasi-static loading condition from small to large deformation.

Figure 4 shows the simulation data at low-speed crushing compared with the model calculation. A good agreement between two results is observed which validates the effectiveness of the model.

### *Two-phase model for impact*

The mechanical behaviors of buckyball during the first phase at both low-speed crushing and impact loadings are similar. Thus, Equation 2 is still valid in phase I with a different $f^* \approx 4.30$. The characteristic buckling time, the time it takes from contact to buckle, is on the order of $\tau \approx 10^{-1} \sim 10^{0}$ ns $\sim T \approx 2.5R/c_1 \approx 5.71 \times 10^{-5}$ns, where $\rho$ is the density of $C_{720}$ and $c_1 = \sqrt{E/\rho}$. It is much longer than the wave traveling time; thus, the enhancement of $f^*$ should be caused by the inertia effect [43].

As indicated before, the buckyball behaves differently during the post-buckling phase if it is loaded dynamically, i.e., no obvious snap through would be observed at the buckling point such that the thin spherical structure is able to sustain load by bending its wall. Therefore, a simple shell bending model is employed here to describe its behavior as shown in Figure 3; the top and bottom flattened wall with length of $L$ experiences little stretching strain, whereas the side wall bends with finite deformation, governing the total system strain energy

$$E_{\text{system}} = \frac{1}{2}\int_A \frac{M^2}{EI} dA \tag{11}$$

where the bending rigidity $EI = \frac{Eh'^3}{12(1-\nu^2)}$ and $M$ is the bending moment. $A$ denotes the integration area. The $h'$ is the 'enlarged' thickness, the result of smaller snap-through phenomenon. Here, $h' \approx 1.40h$ via data fitting. Substituting geometrical constraints and taking

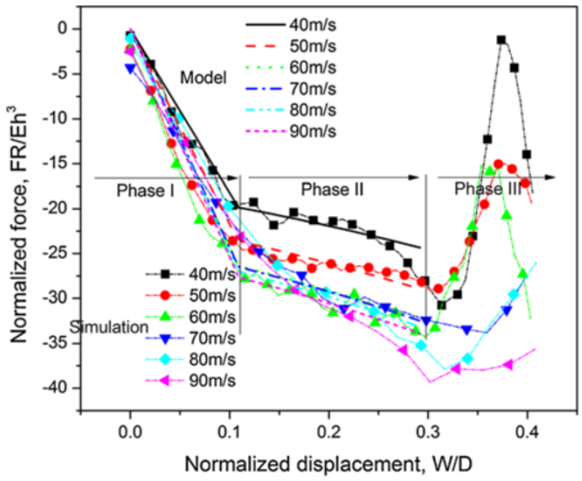


**Figure 5 Comparison between computational results and analytical model.** Comparison between computational results and analytical model at various impact speeds from 40 to 90 m/s.

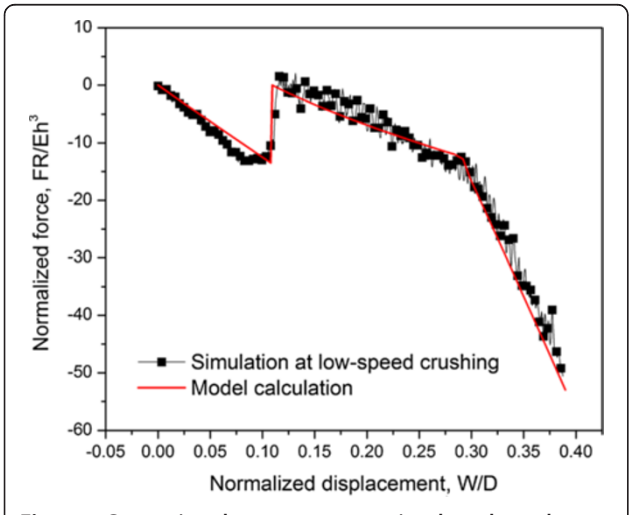


**Figure 4 Comparison between computational results and analytical model at low-speed crushing of 0.01 m/s.**

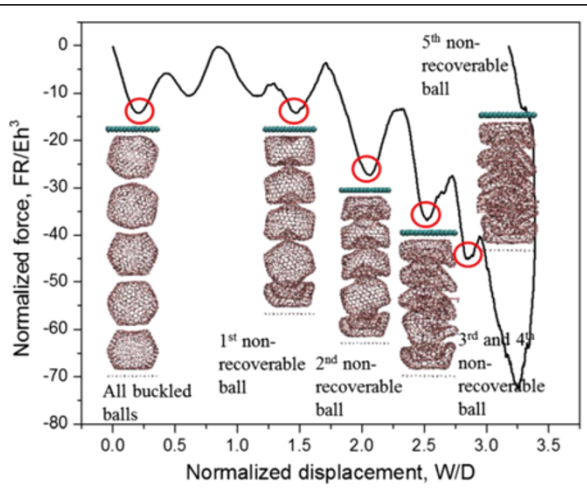


**Figure 6 Characteristic normalized force-displacement curve of 1-D system with vertically lined $C_{720}$ buckyballs.** The characteristic normalized force-displacement curve of 1-D system with five vertically lined $C_{720}$s at impact speed of 50 m/s.

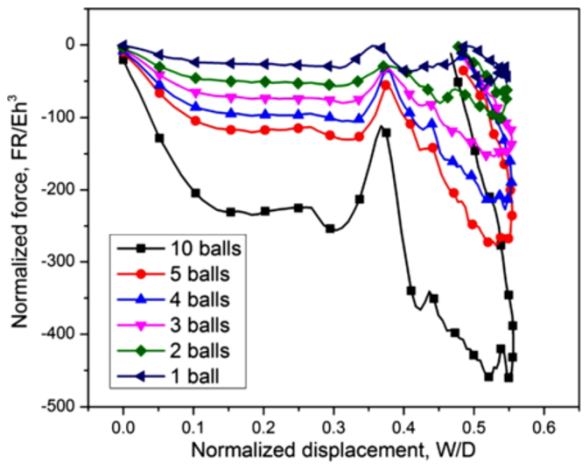


**Figure 7 Characteristic normalized force-displacement curve of 1-D buckyball system with various numbers of horizontally lined $C_{720}$ buckyballs.** The characteristic normalized force-displacement curve of 1-D buckyball system with various numbers of horizontally lined $C_{720}$s at impact speed of 50 m/s.

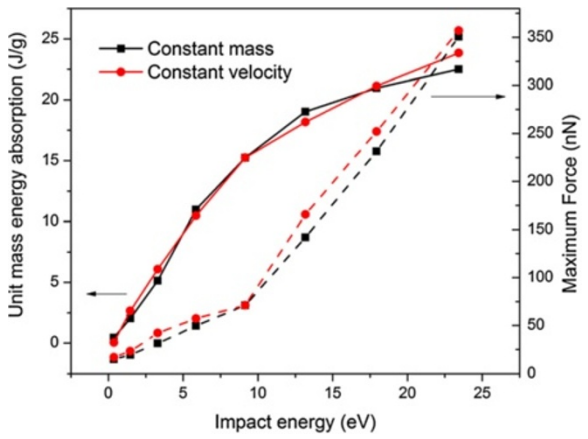


**Figure 9 UME and maximum contact force at constant impact speed (50 m/s) with various impact masses.** UME and maximum contact force at constant impact speed (50 m/s) with various impact mass (from $8.7 \times 10^{-19}$ to $7.1 \times 10^{-17}$ g), and constant impact mass ($2.8 \times 10^{-18}$ g) with various impact speeds (from 10 to 90 m/s), for five-buckyball systems.

the derivative, the force-displacement relation becomes (for $C_{720}$ under 100 m/s impact)

$$F_2 = \frac{1}{4} EI \frac{1}{(R - W_2/2)^2} \pi^2 \cdot \pi R \quad (W_{b1} < W_2 \le W_{b2}) \tag{12}$$

Therefore, Equations 3 and 12 together provide a model to describe the mechanical behavior of the buckyball under dynamic loadings.

When the impact speed is varied, the corresponding force is modified by a factor $\alpha$ owing to strain rate effect [44-46]. With the subscript representing the impact speed (in units of m/s), the correction factor $\mathbf{c} = [\alpha_{40}, \alpha_{50}, \alpha_{60}, \alpha_{70}, \alpha_{80}, \alpha_{90}] = [0.83, 1.00, 1.12, 1.14, 1.17]$. Figure 5 illustrates the comparison between atomistic simulation and model (for impact speeds of 40 to 90 m/s), with good agreements.

## Results and discussion

### Buckyball assembly

In practice, buckyballs need to be assembled (shown in Figure 1) so as to protect materials/devices. Various stacking arrays are investigated as follows.

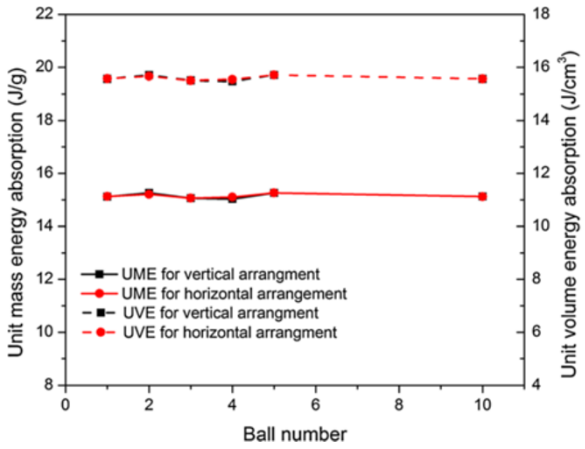


**Figure 8 UME and UVE values of both vertical and horizontal buckyball systems with various buckyball numbers.** UME and UVE values of both vertical and horizontal buckyball systems with various buckyball numbers at impact speed of 50 m/s.

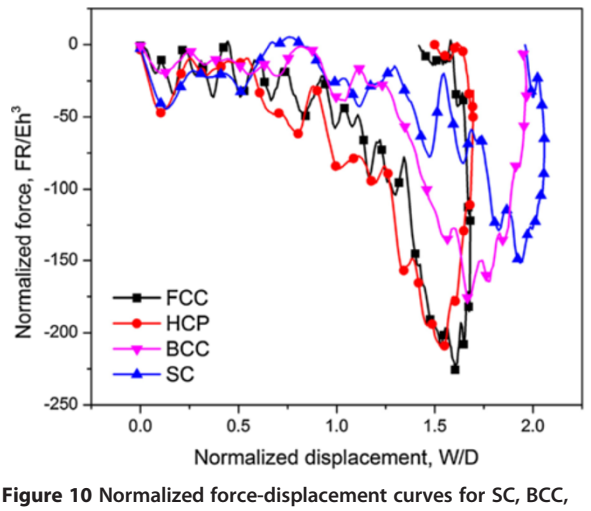


**Figure 10 Normalized force-displacement curves for SC, BCC, FCC and HCP packing of $C_{720}$.** Typical normalized force-displacement curves for SC, BCC, FCC and HCP packing of $C_{720}$ at impact speed of 50 m/s, and the impact energy per buckyball is 1.83 eV.

### 1-D alignment buckyball system

The $C_{720}$ can be arranged both vertically and horizontally in a 1-D chain-like alignment. Figure 6 shows the mechanical behavior of a five-buckyball array subjecting to a rigid plate impact with impact energy and speed of 9.16 eV and 50 m/s respectively. Progressive buckling and bowl-shape forming behavior takes the full advantage of single buckyball energy absorption ability one by one and controls the force on the receiver within a relatively low value during first section of deformation (within $W/D < 1.5$) which provides cushion protections.

Another 1-D arrangement direction is normal to a plate impact. Unlike the progressive buckling behavior in the vertical system, all buckyballs buckle simultaneously in the horizontal array. Figure 7 shows the scenario with impact energy of 1.83 eV per buckyball and impact speed of 50 m/s, where the total reaction force scales with the number of buckyballs. Systems with different buckyball numbers show almost uniform deformation characteristics of individual buckyballs.

The energy absorption per unit mass (UME, J/g) and unit volume (UVE, J/cm$^3$) are given in Figure 8, which shows that the UME and UVE are almost invariant regardless of buckyball number or arrangement. In Figure 8 the impact energy per buckyball is fixed as 1.83 eV; if the impact energy or speed changes, the value of UME or UVE alters; however, the result is still insensitive to buckyball number or arrangement. The major responsible

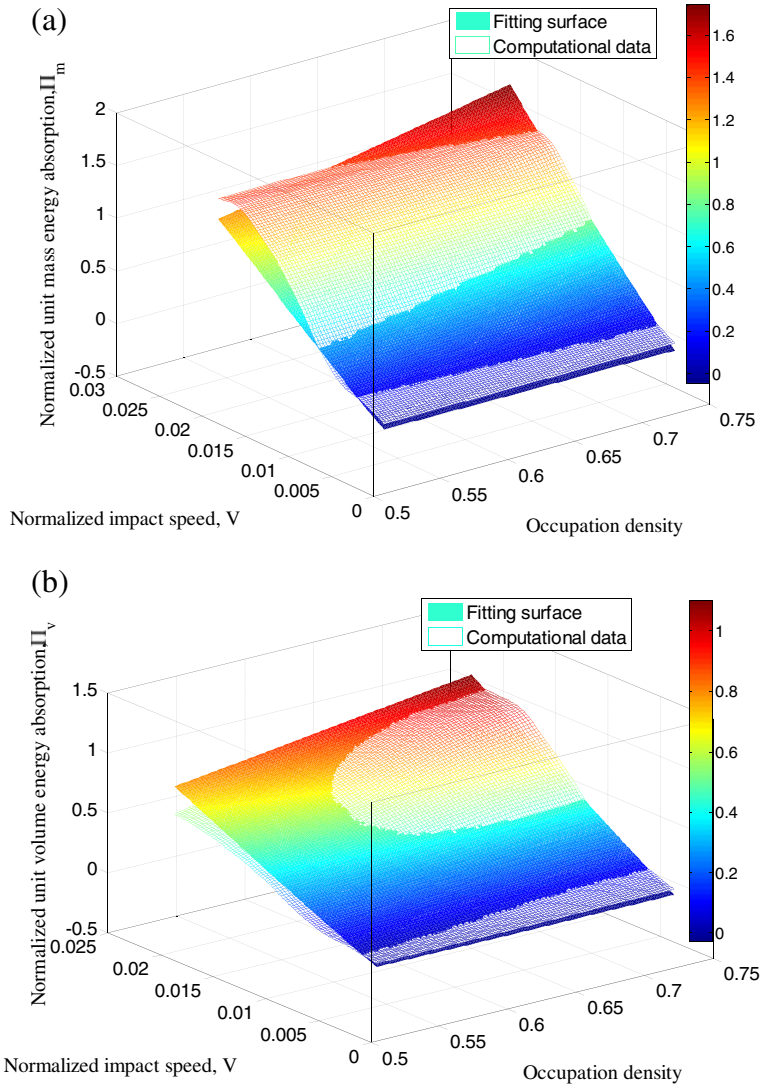


**Figure 11 UME and UVE values of SC, BCC, FCC, and HCP packing of $C_{720}$ at impact speeds.** UME and UVE values of SC, BCC, FCC, and HCP packing of $C_{720}$ at impact speeds from 10 m/s to 90 m/s. Fitting surfaces based on the empirical equations are also compared with the simulation. (**a**) UME values of various packing forms of $C_{720}$ at impact various impact speeds. (**b**) UVE values of various packing forms of $C_{720}$ at impact various impact speeds.

reason is that the energy absorption ability of the system stems from the non-recoverable deformation of individual buckyball which is almost uniform.

By fixing either the impact speed or mass and varying the other parameter, the impact energy per buckyball can be varied. It imposes a nonlinear influence on the UME and the maximum force on the receiver, as shown in Figure 9 for the vertical alignment of five-buckyball system. No matter how the impact speed or mass varies, it is the impact energy per buckyball that dominates the values of UME and maximum transmitted force.

#### *3-D stacking buckyball system*

The packing density of a 3-D stacking system can be different than that of the 1-D system, and thus the performance is expected to vary. Four types of 3-D stacking forms are investigated, i.e., simple cubic (SC), body-centered cubic (BCC), face-centered cubic (FCC) (a basic crystal structure of buckyball [47]), and hexagonal-closed packing (HCP). The occupation density $\eta_{SC} = \pi/6 \approx 0.52$, $\eta_{BCC} = \pi\sqrt{3}/8 \approx 0.68$, $\eta_{\mathrm{FCC}} = \eta_{\mathrm{HCP}} = \pi/3\sqrt{2} \approx 0.74$ [48] for SC, BCC, FCC, and HCP, respectively. Convergence study indicates that the profiles of force-displacement curves as well as the energy absorption rate at increasing buckyball numbers at one computational cell keep the same. In this case, a fundamental unit, such as containing 2 × 2 × 3 buckyballs for SC arrangement is shown in Figure 1c.

Figure 10 illustrates the normalized force-displacement curves for SC, BCC, FCC, and HCP units under the same impact energy per buckyball (1.83 eV). As expected, the mechanical behaviors of FCC and HCP are similar, while the BCC and SC units (with lower $\eta$) have more space for system to comply and hence the impact force is smaller yet the displacement is larger. Consequently, FCC and HCP have the same energy absorption ability and that of BCC and SC are inferior.

Energy absorption performances of the three basic units are studied at various impact speeds, i.e., from 10 to 90 m/s while the impact mass is kept a constant, as shown in Figure 11. With the impact speed increases, more mechanical energy is absorbed; but the increasing trend becomes slighter at higher impact speed when the buckyball system reaches its mitigation limit. The improvement is greater in terms of UVE than UME with higher $\eta$.

By normalizing the UME and UVE as $\Pi_{\mathrm{m}}$ = UME/($E_{\mathrm{impactor}}/m$) and $\Pi_v$ = UVE/($E_{\mathrm{impactor}}/V_{\mathrm{volume}}$) where $V_{\mathrm{volume}}$ is the volume of the buckyball and impact speed as $V = v/\sqrt{B/\rho}$ where $B$ = 34 GPa [49] is the bulk modulus of graphite. An empirical equation could be fitted as

$$\Pi_m = A\eta\left(BV^C + DV\right) \tag{13}$$

where $A$ = 5.50, $B$ = −0.25, $C$ = 0.21, and $D$ = 25.0 with fitting correlation coefficient of 0.96 and

$$\Pi_v = A\eta\left(BV^C + DV\right), \tag{14}$$

where $A$ = 0.46, $B$ = −1.94, $C$ = 0.21, and $D$ = 187.9 with fitting correlation coefficient of 0.96. These equations are valid for low-speed impact speed (below 100 m/s) on stacked $C_{720}$ buckyballs. When the impact speed is fixed, the unit energy absorption linearly increases with the occupation density; under a particular spatial arrangement, the energy absorption ability increases nonlinearly with the impact speed.

## Conclusions

$C_{720}$ as a representative giant buckyball has the distinctive property of non-recovery deformation after crushing or impact, which makes it capable of absorbing a large amount of energy. The mechanical behaviors of a single $C_{720}$ under quasi-static (low-speed crushing) and dynamic impact are investigated via MD simulation and analytical modeling. By understanding the mechanism of mechanical behavior of individual $C_{720}$, the energy absorption ability of a 1-D array of buckyball system is studied. It is found that regardless of the direction of alignment and number of buckyballs, the unit energy absorption density is almost the same for low-speed impact. In addition, different 3-D stacking at various impact speeds and stacking forms are investigated. Explicit empirical models are suggested where packing density and impact speed may pose a positive effect on the unit energy absorption. This study may shed lights on the buckyball dynamic mechanical behavior and its application in energy absorption devices and inspire the related experimental work.

#### Competing interests

The authors declare that they have no competing interests.

#### Authors' contributions

JX carried out the molecular dynamic simulation and drafted the manuscript. YL participated in the design of the study and performed the mechanical analysis. XC and YX conceived of the study and participated in its design and coordination and helped draft the manuscript. All authors read and approved the final manuscript.

#### Authors' information

JX is a Ph.D. candidate in Department of Earth and Environmental Engineering at Columbia University, supported by the Presidential Distinguished Fellowship. His research interests are nanomechanics and energy-related materials. YL is a Professor in Department of Automotive Engineering at Tsinghua University. He has been awarded by the National Science and Technology Advancement Award (second prize) for twice. His major research interests are advanced energy absorption material. YX is a Professor in School of Energy Science and Engineering at University of Electronic Science and Technology of China. His research is focused on combinatorial materials research with emphasis on energy applications, particularly on thin film materials and devices, printed electronics, and power electronics. He has authored and co-authored more than 40 articles, with an *h*-index of 12. XC is an Associate Professor in Department of Earth and Environmental Engineering at Columbia University. He uses multiscale

theoretical, experimental, and numerical approaches to investigate various research frontiers in materials addressing challenges in energy and environment, nanomechanics, and mechanobiology. He has published over 200 journal papers with an *h*-index over 30.

**Acknowledgments**
The work is supported by National Natural Science Foundation of China (11172231 and 11102099), DARPA (W91CRB-11-C-0112), National Science Foundation (CMMI-0643726), International joint research project sponsored by Tsinghua University (20121080050), Individual-research founding State Key Laboratory of Automotive Safety and Energy, Tsinghua University (ZZ2011-112), and World Class University program through the National Research Foundation of Korea (R32-2008-000-20042-0).

**Author details**
[1]Columbia Nanomechanics Research Center, Department of Earth and Environmental Engineering, Columbia University, New York, NY 10027, USA. [2]State Key Laboratory of Automotive Safety and Energy, Department of Automotive Engineering, Tsinghua University, Beijing 100084, People's Republic of China. [3]State Key Lab of Electronic Thin Films and Integrated Devices, School of Energy Science and Engineering, University of Electronic Science and Technology of China, Chengdu, Sichuan 611731, People's Republic of China. [4]Department of Civil and Environmental Engineering, Hanyang University, Seoul 133-791, South Korea. [5]International Center for Applied Mechanics, SV Lab, Xi'an Jiaotong University, Xi'an 710049, People's Republic of China.

Received: 7 December 2012 Accepted: 16 January 2013
Published: 29 January 2013

**References**

1. Sun LY, Gibson RF, Gordaninejad F, Suhr J: **Energy absorption capability of nanocomposites: a review.** *Compos Sci Technol* 2009, **69:**2392–2409.
2. Barnat W, Dziewulski P, Niezgoda T, Panowicz R: **Application of composites to impact energy absorption.** *Comp Mater Sci* 2011, **50:**1233–1237.
3. Deka LJ, Bartus SD, Vaidya UK: **Damage evolution and energy absorption of E-glass/polypropylene laminates subjected to ballistic impact.** *J Mater Sci* 2008, **43:**4399–4410.
4. Mylvaganam K, Zhang LC: **Energy absorption capacity of carbon nanotubes under ballistic impact.** *Appl Phys Lett* 2006, **89:**123–127.
5. Xu J, Li YB, Chen X, Ge DY, Liu BH, Zhu MY, Park TH: **Automotive windshield - pedestrian head impact: energy absorption capability of interlayer material.** *Int J Auto Tech-Kor* 2011, **12:**687–695.
6. Wang DM: **Impact behavior and energy absorption of paper honeycomb sandwich panels.** *Int J Impact Eng* 2009, **36:**110–114.
7. Xu J, Xu B, Sun Y, Li Y, Chen X: **Mechanical energy absorption characteristics of hollow and water-filled carbon nanotubes upon low speed crushing.** *J Nanomechanics Micromechanics* 2012, **2:**65–70.
8. Weidt D, Figiel L, Buggy M: **Prediction of energy absorption characteristics of aligned carbon nanotube/epoxy nanocomposites.** *IOP Conf Ser Mater Sci Eng* 2012, **40**(1):012028.
9. Lu W, Punyamurtula VK, Qiao Y: **An energy absorption system based on carbon nanotubes and nonaqueous liquid.** *Int J Mat Res* 2011, **102:**587–590.
10. Zhang Q, Zhao MQ, Liu Y, Cao AY, Qian WZ, Lu YF, Wei F: **Energy-absorbing hybrid composites based on alternate carbon-nanotube and inorganic layers.** *Adv Mater* 2009, **21:**2876-+.
11. Gui XC, Wei JQ, Wang KL, Cao AY, Zhu HW, Jia Y, Shu QK, Wu DH: **Carbon nanotube sponges.** *Adv Mater* 2010, **22:**617-+.
12. Wang CM, Zhang YY, Xiang Y, Reddy JN: **Recent studies on buckling of carbon nanotubes.** *Appl Mech Rev* 2010, **63:**030804.
13. Chandraseker K, Mukherjee S: **Atomistic-continuum and *ab initio* estimation of the elastic moduli of single-walled carbon nanotubes.** *Comp Mater Sci* 2007, **40:**147–158.
14. Yakobson BI, Brabec CJ, Bernholc J: **Nanomechanics of carbon tubes: instabilities beyond linear response.** *Phys Rev Lett* 1996, **76:**2511–2514.
15. Cao GX, Chen X: **Buckling behavior of single-walled carbon nanotubes and a targeted molecular mechanics approach.** *Phys Rev B* 2006, **74:**165422.
16. Chesnokov SA, Nalimova VA, Rinzler AG, Smalley RE, Fischer JE: **Mechanical energy storage in carbon nanotube springs.** *Phys Rev Lett* 1999, **82:**343–346.
17. Huhtala M, Krasheninnikov AV, Aittoniemi J, Stuart SJ, Nordlund K, Kaski K: **Improved mechanical load transfer between shells of multiwalled carbon nanotubes.** *Phys Rev B* 2004, **70:**045404.
18. Liu C, Li F, Ma L-P, Cheng H-M: **Advanced materials for energy storage.** *Adv Mater* 2010, **22:**E28-+.
19. Coluci VR, Fonseca AF, Galvao DS, Daraio C: **Entanglement and the nonlinear elastic behavior of forests of coiled carbon nanotubes.** *Phys Rev Lett* 2008, **100:**086807.
20. Daraio C, Nesterenko VF, Jin S, Wang W, Rao AM: **Impact response by a foamlike forest of coiled carbon nanotubes.** *J Appl Phys* 2006, **100:**064309.
21. Daraio C, Nesterenko VF, Jin SH: **Highly nonlinear contact interaction and dynamic energy dissipation by forest of carbon nanotubes.** *Appl Phys Lett* 2004, **85:**5724–5726.
22. Zhenyong M, Zhengying P, Lei L, Rongwu L: **Molecular dynamics simulation of low-energy C60 in collision with a graphite (0001) surface.** *Chinese Phys Lett* 1995, **12:**751.
23. Man ZY, Pan ZY, Ho YK: **The rebounding of C60 on graphite surface: a molecular dynamics simulation.** *Phys Lett A* 1995, **209:**53–56.
24. Pan ZY, Man ZY, Ho YK, Xie J, Yue Y: **Energy dependence of C60-graphite surface collisions.** *J Appl Phys* 1998, **83:**4963–4967.
25. Kaur N, Gupta S, Dharamvir K, Jindal VK: **Behaviour of a bucky-ball under extreme internal and external pressures**. In *26th International Symposium on Shock Waves: July 15-20 2007; Gottingen*. Edited by Hannemann K, Seiler F. Gottingen: Springer; 2009.
26. Zhanga Z, Wanga X, Lia J: **Simulation of collisions between buckyballs and graphene sheets.** *Int J Smart Nano Mat* 2012, **3:**14–22.
27. Wang X, Lee JD: **Heat wave driven by nanoscale mechanical impact between and graphene.** *J Nanomechanics Micromechanics* 2012, **2:**23–27.
28. Xu J, Sun Y, Li Y, Xiang Y, Chen X: **Molecular dynamics simulation of impact response of buckyballs.** *Mech Res Commun*, :. In press.
29. Zope RR, Baruah T, Pederson MR, Dunlap BI: **Static dielectric response of icosahedral fullerenes from C(60) to C(2160) characterized by an all-electron density functional theory.** *Phys Rev B* 2008, **77:**115452.
30. Zope RR, Baruah T: **Dipole polarizability of isovalent carbon and boron cages and fullerenes.** *Phys Rev B* 2009, **80:**033410.
31. Dunlap BI, Zope RR: **Efficient quantum-chemical geometry optimization and the structure of large icosahedral fullerenes.** *Chem Phys Lett* 2006, **422:**451–454.
32. Plimpton S: **Fast parallel algorithms for short-range molecular-dynamics.** *J Comput Phys* 1995, **117:**1–19.
33. Girifalco LA, Hodak M: **Van der Waals binding energies in graphitic structures.** *Phys Rev B* 2002, **65:**125404.
34. Chen X, Huang YG: **Nanomechanics modeling and simulation of carbon nanotubes.** *J Eng Mech-Asce* 2008, **134:**211–216.
35. Huang Y, Wu J, Hwang KC: **Thickness of graphene and single-wall carbon nanotubes.** *Phys Rev B* 2006, **74:**245413.
36. Yang XD, He PF, Gao HJ: **Modeling frequency- and temperature-invariant dissipative behaviors of randomly entangled carbon nanotube networks under cyclic loading.** *Nano Res* 2011, **4:**1191–1198.
37. Updike DP, Kalnins A: **Axisymmetric postbuckling and nonsymmetric buckling of a spherical shell compressed between rigid plates.** *J Appl Mech* 1972, **39:**172–178.
38. Updike DP, Kalnins A: **Axisymmetric behavior of an elastic spherical shell compressed between rigid plates.** *J Appl Mech* 1970, **37:**635–640.
39. Reissner E: **On the theory of thin, elastic shells**. In *Contributions to Applied Mechanics (the H. Reissner Anniversary Volume)*. Ann Arbor: J. W. Edwards; 1949:231–247.
40. Pauchard L, Rica S: **Contact and compression of elastic spherical shells: the physics of a 'ping-pong' ball.** *Philos Mag B* 1998, **78:**225–233.
41. Hubbard M, Stronge WJ: **Bounce of hollow balls on flat surfaces.** *Sports Engineering* 2001, **4:**49–61.
42. Steele CR: **Impact of shells**. In *Fourth Conference on Non-linear Vibrations, Stability, and Dynamics of Structures and Mechanisms: June 1, 1988; Blacksburg*. Edited by Nayfey AH, Mook DT. Blacksburg: Virginia Polytechnic Institute; 1988.
43. Lu G, Yu TX: *Energy Absorption of Structures and Materials*. Cambridge: Woodhead; 2003.
44. Koh ASJ, Lee HP: **Shock-induced localized amorphization in metallic nanorods with strain-rate-dependent characteristics.** *Nano Lett* 2006, **6:**2260–2267.
45. Yi LJ, Yin ZN, Zhang YY, Chang TC: **A theoretical evaluation of the temperature and strain-rate dependent fracture strength of tilt grain boundaries in graphene.** *Carbon* 2013, **51:**373–380.

46. Zhao H, Aluru NR: **Temperature and strain-rate dependent fracture strength of graphene.** *J Appl Phys* 2010, **108:**064321.
47. Ganin AY, Takabayashi Y, Khimyak YZ, Margadonna S, Tamai A, Rosseinsky MJ, Prassides K: **Bulk superconductivity at 38 K in a molecular system.** *Nat Mater* 2008, **7:**367–371.
48. Hilbert D, Cohn-Vossen S: *Geometry and the Imagination.* New York: Chelsea; 1983.
49. Ruoff RS, Ruoff AL: **The bulk modulus of C60 molecules and crystals - a molecular mechanics approach.** *Appl Phys Lett* 1991, **59:**1553–1555.

doi:10.1186/1556-276X-8-54
**Cite this article as:** Xu *et al.*: Energy absorption ability of buckyball $C_{720}$ at low impact speed: a numerical study based on molecular dynamics. *Nanoscale Research Letters* 2013 **8**:54.